Hindawi Publishing Corporation
Journal of Chemistry
Volume 2013, Article ID 359202, 8 pages
http://dx.doi.org/10.1155/2013/359202

Research Article

Adsorption of Trinitrotoluene on a MgO(001) Surface Including Surface Relaxation Effects

Thiago Guerra[1] and Itamar Borges Jr.[1,2]

[1] *Programa de Pós-Graduação em Engenharia de Defesa, Instituto Militar de Engenharia, 80, 22290-270 Rio de Janeiro, RJ, Brazil*
[2] *Departamento de Química, Instituto Militar de Engenharia, Praça General Tibúrcio, 80, 22290-270 Rio de Janeiro, RJ, Brazil*

Correspondence should be addressed to Itamar Borges Jr.; itamar@ime.eb.br

Received 28 June 2012; Revised 31 July 2012; Accepted 31 July 2012

Academic Editor: Cristiano R. W. Guimarães

A thorough investigation of 2,4,6-trinitrotoluene (TNT) adsorption on a MgO(001) surface was carried out using density functional theory (DFT) combined with periodic boundary conditions. Four different initial orientations of the TNT molecule, adsorbed on two different representations of the MgO(001) surface, were investigated. In the first surface representation, there were two fixed layers of atoms and in the second the surface had three layers, with the uppermost fully relaxed in geometry optimizations. Electron density difference maps for each case were computed and provided a detailed picture of the interactions. The results showed a physical adsorption process for both surface representations. In the most favorable situation—TNT adsorbed on the surface with three layers—the computed adsorption energy was −9.89 kcal/mol. The importance of allowing the uppermost layer of the surface to fully relax upon molecular desorption was shown.

1. Introduction

Explosives and propellants—energetic materials—have a large spectrum of military and civilian applications. Investigations of these materials involve complex physical-chemical processes and experimental work can be dangerous. For these reasons, theoretical work on these substances can be especially valuable.

We have been working on several aspects of energetic materials employing a variety of theoretical chemistry/molecular modeling tools. We have focused on excited states [1–4], decomposition processes [5], and sensitivity properties [6, 7]. Concerning catalytic studies, we studied a variety of processes on oxides [8] and layered hydroxides [9, 10]. In this work, we examine a possible role of magnesium oxides in the decomposition of a nitroaromatic explosive, TNT (2,4,6-trinitrotoluene).

TNT (2,4,6-trinitrotoluene) is an explosive material widely used for military and civilian purposes [11]. As a result of widespread use, residual TNT in both soil and groundwater has been detected [12, 13]. In particular, the presence of TNT and its degradation products in aquatic environment was associated with adverse impacts on biological receptors and communities [13, 14]. TNT was listed as a significant pollutant to public health and aquatic life.

TNT-contaminated water can be treated by various methods, including activated carbon adsorption [15, 16], supercritical water oxidation [17], Fenton reagent oxidation [18], and photocatalytic oxidation [19, 20]. In spite of their usefulness for TNT degradation, residual products from these treatments are still potentially harmful.

Magnesium oxide (MgO), also named periclase, is an important mineral with rock-salt structure readily cleaving along the (001) direction, the most stable surface. After cleavage, the terminated surface exposes equal numbers of cations and anions. There is only a slight reconstruction on clean MgO(001) surface, an rumpling of the topmost surface atoms due to different magnitudes of mutual induced polarizations of the Mg^{2+} and O^{2-} ions [21]. In heterogeneous catalysis, several reactions take advantage of acid-basic properties of the MgO surface [8, 22].

DFT cluster models and periodic boundary condition calculations indicated that alkaline oxides such as CaO and BaO chemisorb NO_x species [23–25]. Moreover, adsorption

of NO_2/NO_2, NO/NO_2, or NO/NO molecular pairs was studied, and it was found that a cooperative effect contributes to increase adsorption energy of the pair [26–28]. Although NO and NO_2 are both radicals, thereby being highly reactive, considering the large availability of magnesium oxides for catalytic applications, we could ask if the TNT molecule, having three nitro groups, could favorably adsorb on a MgO (001) surface through a cooperative effect thus leading to possible deactivation. Answer to this question was the main motivation of the present work. We also investigated the effect of different surface models in the adsorption.

2. Theoretical Methods

We used the density functional theory (DFT) [29, 30] combined with periodic boundary conditions and the PW91 generalized gradient approximation (GGA) exchange-correlation functional of Perdew and Wang [31]. The open-source PWSCF package (Quantum-ESPRESSO is a community project for high-quality quantum-simulation software, based on density-functional theory and coordinated by Paolo Giannozzi. See http://www.quantum-espresso.org and http://www.pwscf.org.), employed for all calculations, uses pseudopotentials to describe core electrons, periodic boundary conditions, and plane-wave basis sets.

The convergence criterion for the electronic self-consistent cycle was fixed to 10^{-7} eV per cell. The Kohn-Sham orbitals were expanded in a plane wave basis set with a maximum kinetic energy (ecut) of 40 Ry (544 eV). The Fermi energy was calculated using the Gaussian broadening technique with a smearing parameter of 0.005 Ry. We used the Vanderbilt [32] ultrasoft pseudopotentials for the C, H, O, N, and Mg atoms. For Mg atoms we used a pseudocore scheme including the 2p electrons in the valence shell. The electron density was computed at the Γ point in the first Brillouin zone of the super cell [33].

The MgO primitive cell has two atoms and the following original parameters: $a = b = c = 4.212$ Å, $\alpha = \beta = \gamma = 90^{\circ}$. The starting geometry for optimization of the clean MgO surface was the experimental bulk geometry [34] with Mg–O distances equal 2.106 Å. After geometry optimization, the Mg–O distance converged to 2.104 Å, and this value was used for the reported calculations. The construction of the supercells employed in the calculations was based on this optimized structure. We used periodic slab geometries consisting of three MgO layers with a 5×5 super-cell (a total of 50 atoms per layer with 25 Mg and 25 O atoms); a vacuum layer of 15 Å was added in the "z" direction—this value was found to eliminate spurious interactions between surface replicas generated by the periodic boundary conditions. The supercell angles had the same values of the MgO experimental geometry. For all calculated structures, the super-cell angles and lattice parameters were kept fixed for the two-layer surface, and when a third layer in the uppermost position was added, it was allowed to fully relax along with the adsorbed molecule. For all structures, the equilibrium positions of the nuclei were found by minimizing the total energy.

For all initial TNT geometries, the molecule was placed in a certain orientation above the top face of the super-cell. Four initial adsorption positions were considered to converge the system to local minima, and for all of them, the TNT molecule starting orientation was laid always parallel to the MgO surface. The TNT starting positions were

Position 1. The oxygen atoms of two nitro groups were placed directly above surface magnesium atoms;
Position 2. The molecule was rotated 30° with respect to the previous position;
Position 3. The molecule was rotated 60° with respect to Position 1 of the molecule;
Position 4. At this position, the molecule was positioned in such way that oxygen atoms of one nitro group of the molecule faced the magnesium atoms of the MgO surface.

In order to analyze the contribution of the additional relaxed layer, we carried out two types of calculations. In the first, we optimized the geometry of the adsorbed TNT on a surface containing only two atomic layers, both fixed in bulk positions and not optimized. In the other calculations, we added a third atomic layer which was allowed to fully relax in the optimization process while the other two were kept frozen at their bulk positions.

We relaxed exclusively the uppermost layer in the three layer surface model because only the geometric parameters of this monolayer are affected in molecular adsorption processes and suffer reconstruction. According to low-energy electron diffraction surface experiments, the best model for this surface corresponds to an inward relaxation of no more than 2.5% of the lattice constant in the superficial monolayer and a rumpling of less than about 2% of the O_2^- ions compared to the Mg_2^+ ions [35]. Therefore, our three-layer model is quite realistic, as we have shown before [8].

The adsorption energy (E_{ads}), considering only electronic contributions, was computed according to the total energy difference:

$$E_{ads} = E_{T(TNT/MgO)} - \left[E_{MgO} + E_{TNT}\right]. \quad (1)$$

The electron density difference plots were calculated according to the expression:

$$\rho_{diff}(\mathbf{r}) = \rho_{TNT/surf}(\mathbf{r}) - \rho_{surf}(\mathbf{r}) - \rho_{TNT}(\mathbf{r}). \quad (2)$$

Pictures constructed according to the previous equation depict regions of electronic charge accumulation and depletion, thereby providing a visualization of interactions between the atoms of the system. The electronic density difference $\rho_{diff}(\mathbf{r})$ was calculated for a regularly spaced set of points in the three-dimensional unitary cell. All points where $\rho_{diff}(\mathbf{r}) \geq 0.003\,\text{eV/Å}^3$ were drawn as red, and points where $\rho_{diff}(\mathbf{r}) \leq -0.003\,\text{eV/Å}^3$ were drawn as blue. Similar electronic density difference pictures can be produced from cluster calculations [5], that is, without using periodic boundary conditions.

It is important to note that calculations were extremely demanding computationally due to the size of the TNT molecule and the super-cell. We are unaware of similar adsorption calculations of a molecule as large as TNT.

3. Results and Discussion

3.1. Geometries and Adsorption Energies. The optimized geometry of the isolated TNT molecule, starting structure for adsorption calculations, is shown in Figure 1. The C–C ring distances have small differences, the largest one being 0.041 Å between the largest (C_2–C_3) and the smallest (C_5–C_6). The largest C–C bond distances involve the C_2 carbon bonded to the methyl group—we have shown before that this atom has the largest site dipole value in TNT [7]. The C–N bonds next to CH_3 are larger by 0.032 Å compared to the other C–N bond. Finally, the N–O bonds differ by only 0.003 Å, with an average bond length of 1.236 Å.

Adsorption calculations starting from an upward TNT position for both types of surfaces did not lead to molecular distortion. This starting orientation was by far the most energetically unfavorable situation; thus it will not be further discussed.

Now we discuss TNT adsorption on the MgO surface with two fixed layers. In Position 1 (Figures 2(a) and 2(b)) the undistorted molecule converged to a distance of 3.4 Å from the surface compared to the starting distance (2.3 Å)—this convergence to farther distances happened in all cases (reported distances refer to the atom closest to the surface, which may differ depending on the situation). An NO_2 group was the closest to the surface, thus having the largest interaction. The adsorption distance from Position 2 (Figures 2(c) and 2(d)) is 3.1 Å, but TNT in this case suffered an appreciable distortion. The electron-withdrawing nitro groups deformed distinctly depending on the surface site. Most of the molecule-surface interaction occurs between TNT electronegative oxygen atoms and Mg^{2+} acid surface sites; TNT oxygen atoms at the same time are repelled by the O_2^- basic sites. The ring and the CH_3 group were also distorted by the surface interaction.

From Position 3, the molecule adsorbed at a separation distance of 3.3 Å (Figures 2(e) and 2(f)) while from Position 4 adsorbed at 3.2 Å. In both cases, similar to Position 1 adsorption, the molecule almost did not suffer distortion. From calculated electronic adsorption energies, TNT adsorption on the 2-layer surface had the following order of decreased stability: 4 (−5.48 kcal/mol), 1 (−5.38 kcal/mol), 3 (−4.26 kcal/mol) and 2 (−3.07 kcal/mol).

TNT adsorption on the three-layer model surface, with the uppermost fully relaxed in geometry optimizations, had some differences compared to the two-layer case. The converged molecule-surface distances for TNT adsorption on the three-layer surface are akin to the two layer case, with final molecule-surface distances around 3.3 Å.

Adsorption from Position 1 (Figures 3(a) and 3(b)) is rather similar in comparison to the two-layer surface, but with important differences: the molecule adsorbed with the ring more planar and the CH_3 group less distorted, both resembling more the initial geometry. On the other hand, the NO_2 groups showed larger distortion, thus indicating their greater interaction with the first layer of the surface, now allowed to fully relax. For Position 2 adsorption (Figures 3(c) and 3(d)), similar to Position 1, the ring planarity was also maintained, but with the molecular orientation more parallel to the surface. In comparison to the two-layer case, the nitro groups were less torsioned though the methyl group distorted considerably, the latter effect probably due to a more favorably position of the methyl hydrogen atoms in relation to the O^{2-} surface atoms.

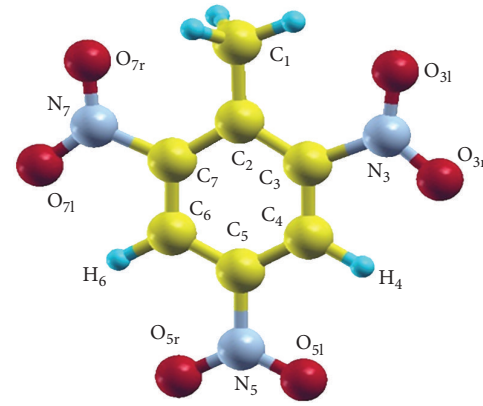

Figure 1: DFT-optimized TNT molecular geometry.

For Position 3 adsorption on the three-layer surface (Figures 3(e) and 3(f)), the molecule preserved its quite symmetrical geometry: the ring remained planar and the nitro groups next to the methyl group were practically symmetrical, both torsioned in the same direction. The methyl group bent in a way to have one of its hydrogen atoms pointing to an O^{2-} surface site and the other H atom converged to a position above the ring. Compared to the two-layer case, the methyl group suffered a considerable distortion. Finally, for Position 4 adsorption (Figures 3(g) and 3(h)) both the nitro and methyl groups deformed, the same happening with the carbon ring; three oxygen atoms of distinct nitro groups converged to a position maximizing their interaction with Mg^{2+} surface sites.

In general, it could be noticed that the largest effect for TNT adsorbed on MgO(001) was the interaction of nitro groups with the surface. The NO_2 group mostly interacting with the surface had the largest C–N distances, a further indication of weakening of these bonds.

The computed electronic adsorption energies for the three layer surface were in order of decreased stability: 1 (−9.80 kcal/mol), 4 (−9.72 kcal/mol), 3 (−9.09 kcal/mol), and 2 (−7.82 kcal/mol). The first three figures are rather similar, virtually identical for starting Positions 1 and 4, all of them characteristic of physisorption. For two-layer surface adsorption, Position 4 was more stable with Position 1 following just the reversed order of the three-layer surface case. Moreover, the adsorption energies for the two-layer surface are about half the values of the three-layer case, thereby displaying the importance of including a third uppermost relaxed layer.

3.2. Electronic Density Differences for TNT Adsorption on the Three-Layer Surface. The analysis of the electronic density

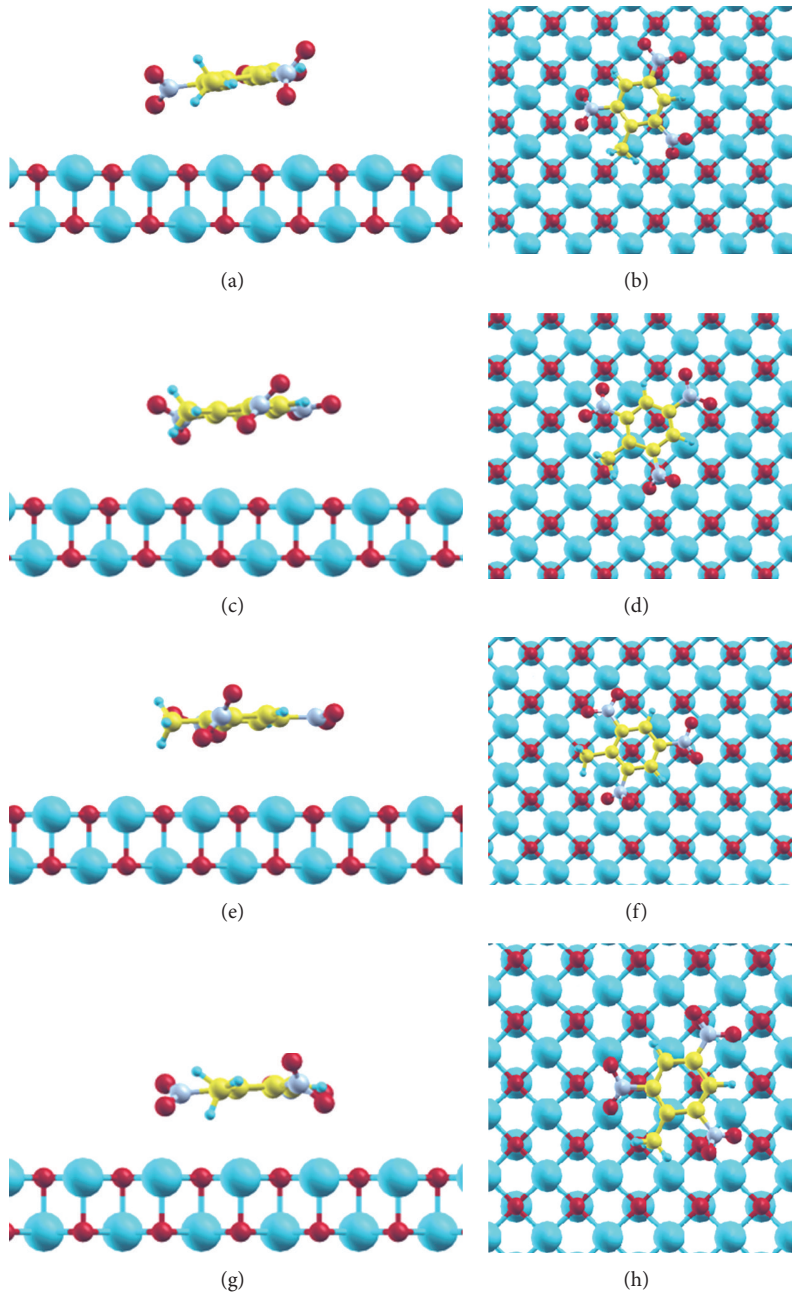

Figure 2: Converged geometries of the TNT molecule adsorbed on the MgO(001) surface with two fixed layers. (a) side view and (b) up view of Position 1; (c) Side view and (d) up view of Position 2; (e) side view and (f) up view of Position 3; (g) side view and (h) up view of Position 4.

difference provides a detailed picture of interactions in the adsorption process.

For Position 1 adsorption (Figure 4(a)), the most favorable energetically for adsorption on the three-layer surface, there is a molecular polarization induced by the surface, present in all TNT atoms but with electron accumulation concentrated on the neighborhood of the electron-withdrawing nitro groups and electron depletion below the ring. On the other hand, the TNT molecule considerably polarized the surface, especially the first layer close to the molecule, thus depleting the surface of electrons. The surface was also similarly polarized for the other three adsorption positions.

In Position 2 (Figure 4(b)), the molecule is rather parallel to the surface and all TNT atoms are polarized. In contrast to Position 1, there is in Position 2 adsorption a remarkable electron accumulation at the top of the atoms, farther from the surface. Below the ring there is considerable electron depletion and, in contrast with Position 1, electron accumulation below the ring, closer to the surface. The strongest interactions, indicated by charge accumulation, are localized

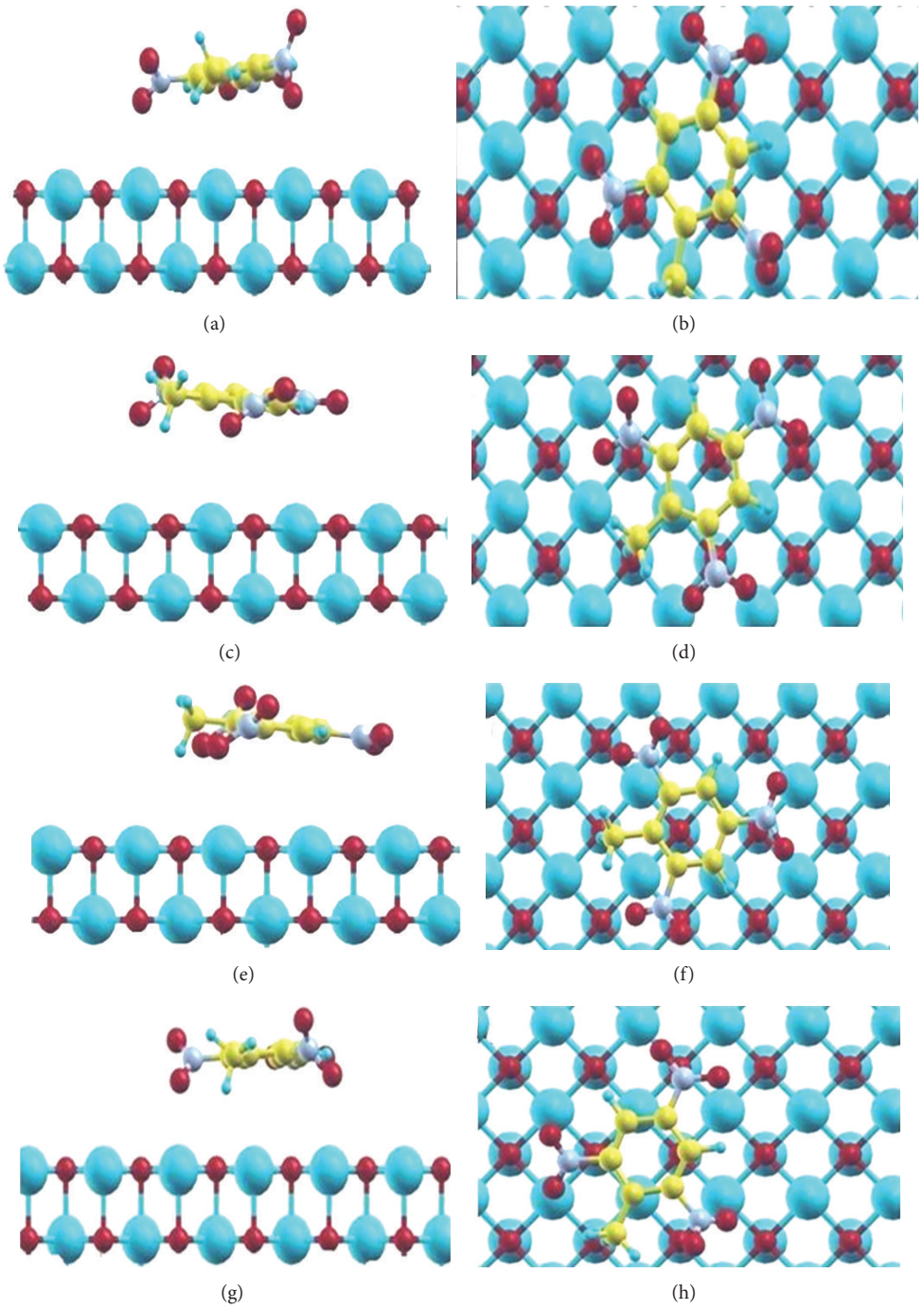

Figure 3: Converged geometries of the TNT molecule above the MgO(001) surface: three layer surface, uppermost layer fully relaxed. (a) side view and (b) up view of position 1; (c) side view and (d) up view of position; (e) side view and (f) up view of position 3 and; (g) side view and (h) up view of position 4.

on the nitro groups next to the methyl group, with the remaining nitro group, distinctive of Position 1 adsorption, having a region of electron depletion around it. These patterns of electronic density explain the fact that adsorption from Position 2 is the less favorable energetically.

In Position 3 (Figure 4(c)), one of the nitro groups, due to greater proximity of the surface, interacts more strongly with Mg^{2+} ionic sites. There is electron depletion on the nitro group opposed to the methyl group and as well below the ring.

Adsorption from Position 4 was energetically the most favorable for the two-layer surface; this situation changed for the three-layer surface, being now the second most stable, energetically close (or rather indistinguishable) to the most stable (Position 1). All TNT atoms for Position 4

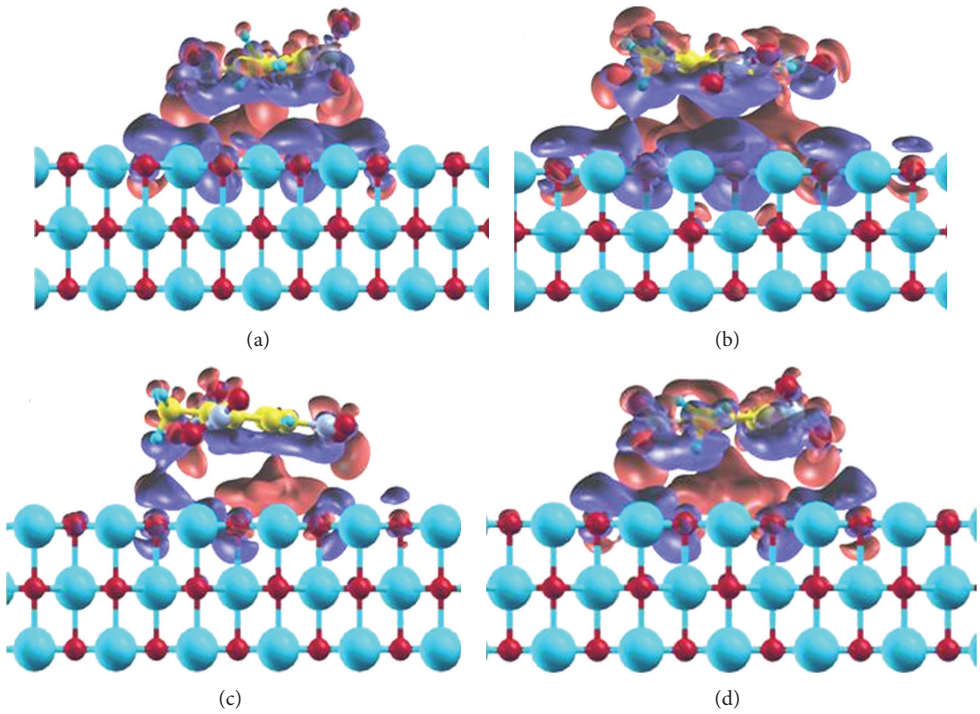

Figure 4: Electronic charge density of the systems adsorbed on the MgO surface with three layers, the uppermost fully relaxed. (a) Side view of Position 1; (b) side view of Position 2; (c) side view of Position 3; (d) side view of Position 4. Blue color indicates regions of charge accumulation while red ones indicate charge depletion.

adsorption were polarized, especially the nitro groups next to the methyl group and the methyl group itself, there was also electron depletion below the ring, and the surface was also polarized. This situation, as expected, was not very different for adsorption from Position 1.

4. Conclusion

In this work we studied adsorption of a TNT molecule on a MgO(001) surface using DFT methods combined with periodic boundary conditions. Electronic adsorption energies and electron density difference maps were computed. A large 5×5 super-cell was necessary to represent accurately the surface. We investigated desorption from four different initial positions of the TNT molecule and two different representations of the surface, one with two fixed layers of atoms and the other one with three layers, the uppermost being fully relaxed, thereby allowing a thorough investigation of TNT adsorption processes on MgO(001).

In other (unpublished) work, calculations of TNT adsorption on a fully optimized $Mg_{36}O_{36}$ model cluster resulted in adsorption energies about six times larger than present values, thus confirming the importance of an accurate representation of the surface for adsorption studies. We particularly stress here the crucial role played by the Madelung (i.e., long range) potential in the description of the surface, adequately included in the present work.

Overall, the adsorbed molecules converged to a molecule-surface distance of about 3.3 Å. We showed that the presence of an uppermost fully relaxed layer in the three-layer surface representation led to important differences when compared to adsorption on the surface with two fixed layers.

The computed electronic adsorption energies, converged molecule-surface adsorption distances, and electron density difference maps characterized a typical physisorption process, which is dominated by dispersion interactions. The electron density difference maps showed differences and similarities depending on the converged adsorption geometries. For instance, the most stable three-layer adsorptions (Position 1 and Position 4), very close in energy, showed similar features in their electron density difference plots: all atoms, especially the nitro groups, were considerably polarized and there was electron depletion below the molecular ring.

We have shown in this work that TNT desorption on MgO(001) is governed by physical interactions. Despite previous evidence of cooperative effects favoring NO_2 and chemisorption of similar small molecules on a MgO(001) surface, contrary to our initial expectations, a similar behavior was not found for TNT (with has three nitro groups) adsorption on the same surface. Therefore, although the MgO(001) catalyst did not present a cooperative effect, further theoretical investigations should be done in order to confirm the role of the MgO(001) surface in TNT deactivation. In spite of that, we have showed that the wealth of information DFT calculations, combined with periodic

boundary conditions, can provide for desorption studies of such large molecules as TNT.

Acknowledgments

This work has been supported by the Brazilian agencies CNPq, Faperj, and CAPES. The authors thank especially Professor M. A. C. Nascimento (UFRJ, Brazil) for providing computer resources for some calculations of this work.

References

[1] I. Borges, "Excited electronic and ionized states of N,N-dimethylnitramine," *Chemical Physics*, vol. 349, no. 1–3, pp. 256–262, 2008.

[2] I. Borges, "Excited electronic and ionized states of the nitramide molecule, H_2NNO_2, studied by the symmetry-adapted-cluster configuration interaction method ," *Theoretical Chemistry Accounts*, vol. 121, no. 5-6, pp. 239–246, 2008.

[3] I. Borges, A. J. A. Aquino, M. Barbatti, and H. Lischka, "The electronically excited states of RDX (hexahydro-1,3,5-trinitro-1,3,5- triazine): vertical excitations," *International Journal of Quantum Chemistry*, vol. 109, no. 11, pp. 2348–2355, 2009.

[4] I. Borges, M. Barbatti, A. J. A. Aquino, and H. Lischka, "Electronic spectra of nitroethylene," *International Journal of Quantum Chemistry*, vol. 112, no. 4, pp. 1225–1232, 2012.

[5] T. F. Moraes and I. Borges, "Nuclear fukui functions and the deformed atoms in molecules representation of the electron density: application to gas-Phase RDX (hexahydro-1,3,5-trinitro- 1,3,5- triazine) electronic structure and decomposition," *International Journal of Quantum Chemistry*, vol. 111, no. 7-8, pp. 1444–1452, 2011.

[6] I. Borges, "Conformations and charge distributions of diazocyclopropanes," *International Journal of Quantum Chemistry*, vol. 108, no. 13, pp. 2615–2622, 2008.

[7] G. Anders and I. Borges, "Topological analysis of the molecular charge density and impact sensitivy models of energetic molecules," *The Journal of Physical Chemistry A*, vol. 115, no. 32, pp. 9055–9068, 2011.

[8] R. S. Alvim, I. Borges, D. G. Costa, and A. A. Leitao, "Density-functional theory simulation of the dissociative chemisorption of water molecules on the MgO(001) surface," *The Journal of Physical Chemistry C*, vol. 116, no. 1, pp. 738–744, 2012.

[9] V. S. Vaiss, R. A. Berg, A. R. Ferreira, I. Borges, and A. A. Leitão, "Theoretical study of the reaction between HF molecules and hydroxyl layers of $Mg(OH)_2$," *Journal of Physical Chemistry A*, vol. 113, no. 23, pp. 6494–6499, 2009.

[10] V. S. Vaiss, I. Borges, and A. A. Leitao, "Sarin degradation using brucite," *The Journal of Physical Chemistry C*, vol. 115, no. 50, pp. 24937–24944, 2011.

[11] K. S. Ro, A. Venugopal, D. D. Adrian et al., "Solubility of 2,4,6-trinitrotoluene (TNT) in water," *Journal of Chemical and Engineering Data*, vol. 41, no. 4, pp. 758–761, 1996.

[12] N. J. Duijm and F. Markert, "Assessment of technologies for disposing explosive waste," *Journal of Hazardous Materials*, vol. 90, no. 2, pp. 137–153, 2002.

[13] J. M. Conder, T. W. La Point, J. A. Steevens, and G. R. Lotufo, "Recommendations for the assessment of TNT toxicity in sediment," *Environmental Toxicology and Chemistry*, vol. 23, no. 1, pp. 141–149, 2004.

[14] J. C. Pennington and J. M. Brannon, "Environmental fate of explosives," *Thermochimica Acta*, vol. 384, no. 1-2, pp. 163–172, 2002.

[15] C. Rajagopal and J. C. Kapoor, "Development of adsorptive removal process for treatment of explosives contaminated wastewater using activated carbon," *Journal of Hazardous Materials*, vol. 87, no. 1–3, pp. 73–98, 2001.

[16] J. W. Lee, T. H. Yang, W. G. Shim, T. O. Kwon, and I. S. Moon, "Equilibria and dynamics of liquid-phase trinitrotoluene adsorption on granular activated carbon: effect of temperature and pH," *Journal of Hazardous Materials*, vol. 141, no. 1, pp. 185–192, 2007.

[17] S. J. Chang and Y. C. Liu, "Degradation mechanism of 2,4,6-trinitrotoluene in supercritical water oxidation," *Journal of Environmental Sciences*, vol. 19, no. 12, pp. 1430–1435, 2007.

[18] S. Y. Oh, P. C. Chiu, B. J. Kim, and D. K. Cha, "Enhancing Fenton oxidation of TNT and RDX through pretreatment with zero-valent iron," *Water Research*, vol. 37, no. 17, pp. 4275–4283, 2003.

[19] H. S. Son, S. J. Lee, I. H. Cho, and K. D. Zoh, "Kinetics and mechanism of TNT degradation in TiO_2 photocatalysis," *Chemosphere*, vol. 57, no. 4, pp. 309–317, 2004.

[20] D. C. Schmelling and K. A. Gray, "Photocatalytic transformation and mineralization of 2,4,6-trinitrotoluene (TNT) in TiO_2 slurries," *Water Research*, vol. 29, no. 12, pp. 2651–2662, 1995.

[21] S. Sawada and K. Nakamura, "Theory of surface rumpling in rock-salt structured ionic crystals," *Journal of Physics C*, vol. 12, no. 6, pp. 1183–1193, 1979.

[22] M. L. Bailly, C. Chizallet, G. Costentin, J. M. Krafft, H. Lauron-Pernot, and M. Che, "A spectroscopy and catalysis study of the nature of active sites of MgO catalysts: thermodynamic brønsted basicity versus reactivity of basic sites," *Journal of Catalysis*, vol. 235, no. 2, pp. 413–422, 2005.

[23] M. Miletic, J. L. Gland, K. C. Hass, and W. F. Schneider, "First-principles characterization of NO_x adsorption on MgO," *Journal of Physical Chemistry B*, vol. 107, no. 1, pp. 157–163, 2003.

[24] M. M. Branda, C. Di Valentin, and G. Pacchioni, "NO and NO_2 adsorption on terrace, step, and corner sites of the BaO surface from DFT calculations," *Journal of Physical Chemistry B*, vol. 108, no. 15, pp. 4752–4758, 2004.

[25] C. di Valentin, G. Pacchioni, and M. Bernasconi, "Ab initio molecular dynamics simulation of NO reactivity on the CaO(001) surface," *Journal of Physical Chemistry B*, vol. 110, no. 16, pp. 8357–8362, 2006.

[26] M. Miletic, J. L. Gland, K. C. Hass, and W. F. Schneider, "Characterization of adsorption trends of NO_2, nitrite, and nitrate on MgO terraces," *Surface Science*, vol. 546, no. 2-3, pp. 75–86, 2003.

[27] W. F. Schneider, "Qualitative differences in the adsorption chemistry of acidic (CO_2, SO_x) and Amphiphilic (NO_x) species on the alkaline earth oxides," *The Journal of Physical Chemistry B*, vol. 108, pp. 273–282, 2004.

[28] P. Broqvist, I. Panas, and H. Grönbeck, "The nature of NO_x species on BaO(100): an Ab initio molecular dynamics study," *Journal of Physical Chemistry B*, vol. 109, no. 32, pp. 15410–15416, 2005.

[29] P. Hohenberg and W. Kohn, "Inhomogeneous electron gas," *Physical Review*, vol. 136, no. 3, pp. B864–B871, 1964.

[30] W. Kohn and L. J. Sham, "Self-consistent equations including exchange and correlation effects," *Physical Review*, vol. 140, no. 4, pp. A1133–A1138, 1965.

[31] J. P. Perdew and Y. Wang, "Accurate and simple analytic representation of the electron-gas correlation energy," *Physical Review B*, vol. 45, no. 23, pp. 13244–13249, 1992.

[32] D. Vanderbilt, "Soft self-consistent pseudopotentials in a generalized eigenvalue formalism," *Physical Review B*, vol. 41, no. 11, pp. 7892–7895, 1990.

[33] M. C. Payne, M. P. Teter, D. C. Allan, T. A. Arias, and J. D. Joannopoulos, "Iterative minimization techniques for ab initio total-energy calculations: molecular dynamics and conjugate gradients," *Reviews of Modern Physics*, vol. 64, no. 4, pp. 1045–1097, 1992.

[34] A. F. Wells, *Structural Inorganic Chemistry*, Clarendon Press, Oxford, UK, 5th edition, 1984.

[35] V. E. Henrich and P. A. Cox, *The Surface Science of Metal Oxides*, Cambridge University Press, Cambridge, UK, 1994.